ACS APPLIED MATERIALS & INTERFACES

RESEARCH ARTICLE

www.acsami.org

Interface Enhancement of Glass Fiber Reinforced Vinyl Ester Composites with Flame-Synthesized Carbon Nanotubes and Its Enhancing Mechanism

Lingmin Liao,[†] Xiao Wang,[†,§] Pengfei Fang,[†] Kim Meow Liew,[*,§] and Chunxu Pan[*,†,‡]

[†]School of Physics and Technology and Center for Electron Microscopy, Wuhan University, Wuhan 430072, China

[‡]Key Laboratory of Artificial Micro- and Nano-structures of Ministry of Education, Wuhan University, Wuhan 430072, China

[§]Department of Building and Construction, City University of Hong Kong, Hong Kong, China

ABSTRACT: Interface enhancement with carbon nanotubes (CNTs) provides a promising approach for improving shock strength and toughness of glass fiber reinforced plastic (GFRP) composites. The effects of incorporating flame-synthesized CNTs (F-CNTs) into GFRP were studied, including on hand lay-up preparation, microstructural characterization, mechanical properties, fracture morphologies, and theoretical calculation. The experimental results showed that: (1) the impact strength of the GFRP modified by F-CNTs increased by more than 15% over that of the GFRP modified by CNTs from chemical vapor deposition; and (2) with the F-CNT enhancement, no interfacial debonding was observed at the interface between the fiber and resin matrix on the GFRP fracture surface, which indicated strong adhesive strength between them. The theoretical calculation revealed that the intrinsic characteristics of the F-CNTs, including lower crystallinity with a large number of defects and chemical functional groups on the surface, promoted their surface activity and dispersibility at the interface, which improved the interfacial bond strength of GFRP.

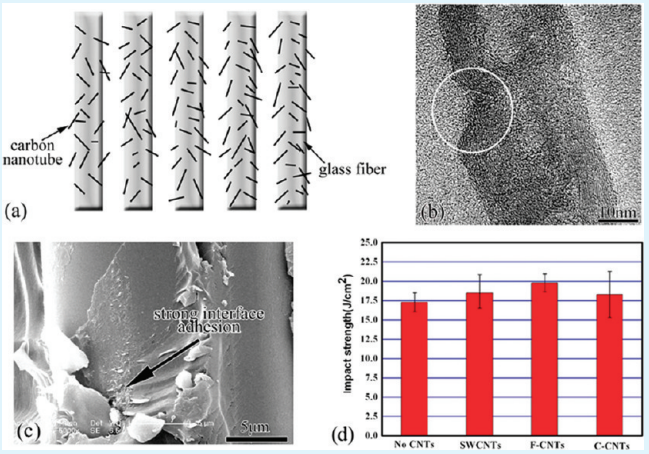

KEYWORDS: carbon nanotubes, glass fiber reinforced plastic, surface characteristics, interface enhancement

1. INTRODUCTION

It is well-known that glass fiber reinforced plastic (GFRP) composites exhibit superior performance combined with high strength, high fatigue resistance, high corrosion resistance and weight reduction compared with regular concrete reinforcing steel bars, and have great potential in construction industry to partially replace steel reinforcement in concrete structures. However, the small elastic modulus and weak ductility of GFRP compared to steel bars make such composites prone to brittle fracture in the presence of large external forces, especially under transverse loading, mainly in the form of delamination between the plies due to the weakness at the fiber/matrix interface. The low shock strength of GFRP thus limits its broader application to stressing reinforcement.

Numerous efforts have been undertaken for improving GFRP to reduce the likelihood of brittle failure caused by poor toughness. Traditionally, several processes have been proposed to enhance its strength and toughness, such as mixing ductile fibers and glass fibers in the GFRP reinforcement phase,[1] or modifying the resin system with toughening agents.[2−4] However, fiber/matrix interfacial debonding is the major mode of failure in GFRP under transverse impact forces; that is, interfacial strength plays a key role in its shock resistance property. Hence, it would be more effective to enhance the interface for improving the toughness and shock resistance of GFRP than to individually modify the fiber or matrix.

The surface treatment of glass fibers with various silane coupling agents is a common method to promote fiber/matrix adhesion and interfacial strength.[5−7] However, the fiber/matrix bond remains weak even after such treatment. Recently, because of the excellent mechanical properties, including high strength, high toughness and large modulus, carbon nanotubes (CNTs) have shown great potential applications in polymer composites.[8−10] Zhu et al[11] at Rice University were the first to develop a process to enhance the interface durability of GFRP using CNTs. They found that the mechanical properties of GFRP were remarkably improved when only 0.015 wt % functionalized single-walled carbon nanotubes (SWCNTs) were added.

However, the widespread use of SWCNTs in GFRP is hindered by their limited supply and high cost. Actually, the

Received: November 15, 2010
Accepted: January 19, 2011
Published: February 3, 2011

nanofillers in polymer composites can be other carbon materials, such as multiwalled carbon nanotubes (MWCNTs),[9,10] graphene,[12,13] and so on. And MWCNTs have become a more attractive and desirable material for practical application in polymer composites. In general, commercial MWCNTs are mainly synthesized using a chemical vapor deposition (CVD) process, but their homogeneous dispersion in polymers is difficult to achieve. Therefore, MWCNTs must be functionalized by utilizing open-end and sidewall chemistry.[14−17] However, such treatments are not only complex to carry out but also difficult to be controlled, and can even destroy the structural and mechanical properties of MWCNTs.[18,19]

In recent years, flame synthesis of CNTs has been considered as a low-cost and potential way to meet mass-production requirements and achieve broader applications. According to our previous work,[20−26] because of special synthesizing conditions in the air, the flame-synthesized CNTs (F-CNTs) possess unique characteristics, such as low crystallinity and a large number of defects on the surface, which yield special optical and electrical properties. It is anticipated that the F-CNTs will also have great potential applications in nanopolymer composites because of their intrinsic reactive surface physical-chemical properties.[27]

In the present work, the F-CNTs were used for the interface enhancement of GFRP. Compared with the commonly used CNTs derived from CVD method, they demonstrated a greater strengthening effect on the interface and more desirable mechanical properties, which made them promising for application in GFRP interface enhancement.

2. EXPERIMENTAL SECTION

The F-CNTs were prepared using ethanol as the carbon source and a pulse-plated Ni nanocrystalline layer upon a copper substrate as the catalyst.[26,28] Because they were grown according to a base growth model and no metal catalyst particles were left on their tips, a purification process using strong acids was not required. For comparison, CNTs derived from a CVD process (C-CNTs and SWCNTs), supplied by Shenzhen Nanotechnologies Co. Ltd., China, were also used for GFRP interface enhancement. The type of glass fibers was ECR 469 L-2400, from Chongqing Polycomp International Corp., China, and the matrix resin was A430 epoxy-based vinyl ester resin, supplied by Jinling DSM Resins Co., Ltd., China. For room temperature curing of the vinyl ester resin, the formulation was: 2 wt % methylethylketone peroxide as the curing agent, 3 wt % cobalt naphthenate as the initiator, and 3 wt % methyl toluidine as the promoter.

The CNT-enhanced GFRP specimens were prepared as follows: (1) the CNTs were dispersed in an ethanol solvent with a concentration of about 0.5 mg/mL and then sonicated in an ultrasonicator (40 kHz) for better dispersion; (2) a spray gun was used to evenly coat the surface of glass fibers with CNTs in ten passes, and the CNT content sprayed was calculated to be roughly 0.021% based on the weight ratio to glass fiber reinforcement; (3) the glass fibers were air-dried at room temperature; (4) pristine glass fibers and those coated with different CNTs were processed into vinyl ester composites using hand lay-up techniques;[29] and (5) after initial room temperature curing for two hours, all specimens were postcured at 100 °C for 1 h to improve the polymerization of GFRP.

The microstructures of the F-CNTs were characterized using a transmission electron microscope (JEOL JEM 2010 TEM, Japan) and high-resolution transmission electron microscope (JEOL JEM 2010FEF HRTEM, Japan). The morphologies of the pristine and the CNT-coated glass fibers were examined using a scanning electron microscope (SIRION SEM, FEI, The Netherlands). The impact strength of the

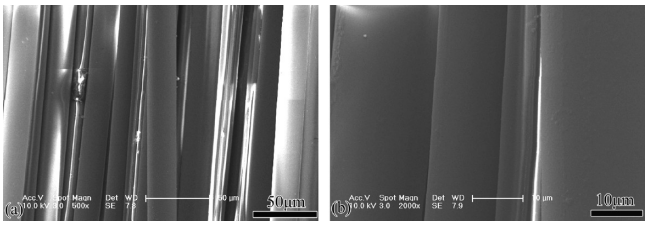

Figure 1. SEM morphology of pristine glass fibers: (a) low magnification; (b) high magnification.

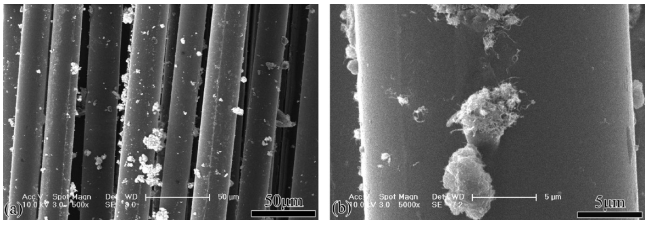

Figure 2. SEM morphology of C-CNT-coated glass fibers: (a) low magnification; (b) high magnification.

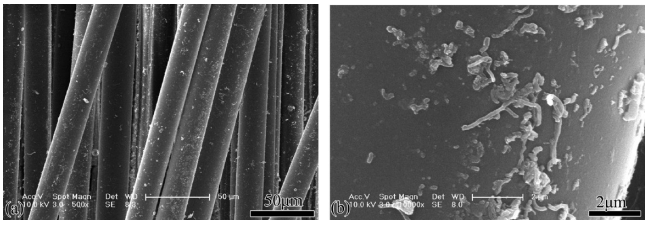

Figure 3. SEM morphology of F-CNT-coated glass fibers: (a) low magnification; (b) high magnification.

GFRP specimens was tested with an MZ-2054 impact testing machine according to GB2571−81 standard (rectangular specimen: 55 × 10 × 4 mm^3, unnotched) of China, in which a transverse load was applied directly at the center of the specimen perpendicular to the fiber direction. The typical impact fracture behavior of each type of GFRP was also analyzed by SEM observation.

The molecular dynamics method[30] was used to implement structural optimization and energy calculations of the F-CNTs and C-CNTs to explain the experimental results. Tetragonal supercells with periodic boundary conditions were adopted. The separation between two neighboring tubes in the $x-y$ plane was 17 Å to avoid interaction between neighboring SWCNTs. The size along the z axis was 9.84 Å, which determined the axial densities of the atom vacancies and chemical groups. The atomic position was relaxed until the forces on the atoms were reduced to within 0.0002 eV/Å.

3. RESULTS AND DISCUSSION

Figure 1 shows SEM images of the smooth and clear surface of the pristine glass fibers. Figures 2 and 3 show the SEM surface morphologies of the glass fibers coated with the C-CNTs and F-CNTs, respectively. The F-CNTs clearly exhibit more preferable dispersity without strong agglomeration on the glass fiber surface compared with the C-CNTs.

Transverse impact testing is an important and credible measurement to examine the mechanical properties, such as strength and toughness of GFRP. The testing results can reflect the influence of effectiveness of the adhesion between glass fiber and resin when stress is transferred at the fiber/matrix interface.

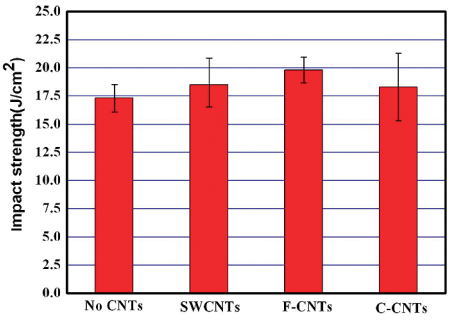

Figure 4. Comparison of the impact strength of GFRP interfacially modified with different carbon nanotubes.

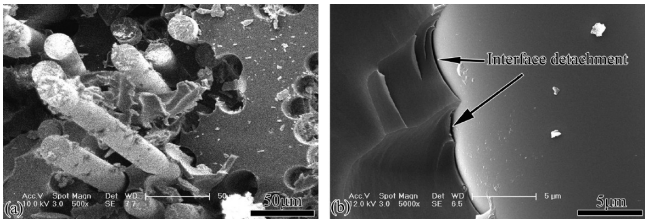

Figure 5. SEM morphologies of (a) transverse failure and (b) unidirectional laminate failure all for the impact fracture of the GFRP without CNT modification.

In addition, the interface integrity is also revealed directly by the impact fracture surface and therefore the interfacial bonding strength of GFRP can be effectively assessed.

Figure 4 illustrates the average values of impact strength of the GFRP for the glass fibers coated with different CNTs. Ten samples were tested for each GFRP specimen with and without CNT enhancement. The results clearly indicate that the GFRP samples with CNT interfacial modification exhibit higher impact strength than those without such modification. Moreover, among different CNTs, F-CNTs improve the impact strength most effectively, by more than 15% over the others.

SEM examinations for impact fracture behavior of the GRFP specimens including the transverse failure surfaces and unidirectional laminate failure surfaces reveal that the impact strength is directly associated with the interfacial bonding between the glass fibers and matrix resin, as shown in Figures 5−7. For example, for the regular glass fiber/resin GRFP without CNT modification, a large number of fibers were pulled out from the resin in a large area and holes are left in the matrix (Figure 5a). In addition, complete detachment of the matrix from the fiber surface is clearly observed (Figure 5b), which implies a weak adhesion at the interface, brittle fracture and the lowest impact strength.

Comparatively, the glass fiber/resin GRFP specimens with CNT modification show a greatly improved interface strength, that is, less fiber pullout and less fiber/matrix debonding. A little residual matrix covering at the fiber surface is also observed, which indicated that the fiber/matrix interfacial strength is greater than the strength of the resin itself. Close SEM observation at high magnification reveals that the CNTs are closely distributed as white dots on the surface of the fibers. However, owing to the limited dispersion, agglomeration of the C-CNTs in some areas of the interface leads to local stress concentration and subsequently, fiber/matrix cracking (Figure 6d). The SWCNT-modified GFRP specimens show the similar interfacial bonding characteristics.

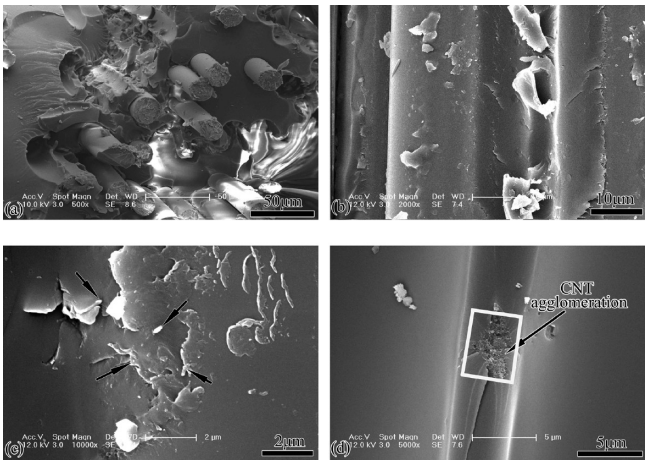

Figure 6. SEM morphologies of (a) transverse failure and (b−d) unidirectional laminate failure all for the impact fracture of the GFRP interfacially modified with C-CNTs.

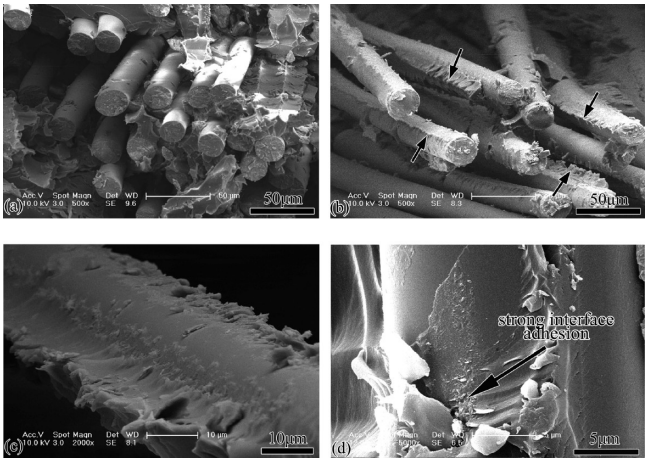

Figure 7. SEM morphologies of (a−c) transverse failure and (d) unidirectional laminate failure all for the impact fracture of the GFRP interfacially modified with F-CNTs.

It is interesting to note that the F-CNT-modified GFRP specimens not only have the highest impact strength but also exhibit a much improved fracture surface and the best interfacial bonding. That is, in addition to the fiber pullout being markedly reduced, a thick layer of resin matrix is also observed covering upon the fiber surface, as shown in Figure 7. More importantly, the increased interfacial strength is due to the good dispersion of the F-CNTs on the fiber surface, as no CNT agglomeration is observed at the interface. Hence, fracture failure does not occur as fiber/matrix interfacial debonding, and the fiber/matrix interface is no longer the weakest part under the transverse impact.

In the fiber-reinforced polymer composites, the fiber/matrix interfacial cohesion directly influences interfacial stress transfer in the composite structure, which thereby significantly affects the integrated mechanical properties. Zhu et al[11] proposed that CNTs enhanced interface durability as follows: (1) CNTs acted as coupling agents in the interphase between the matrix and fiber, and modified the brittleness and toughness of the resin;[31] (2) CNT bundles in the interface were associated with higher energy absorption and could serve to arrest cracks and prevent the expansion of microcracking; and (3) as they were much smaller

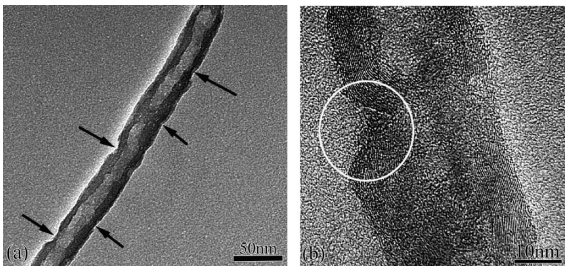

Figure 8. (a) Typical TEM micrograph of an F-CNT; (b) typical HRTEM micrograph of an F-CNT.

than glass fibers, CNTs served to further reinforce the matrix and interface, which could reduce the interlaminar stress concentration by smearing the mismatch of the properties of neighboring plies.[32]

However, it should be noted that the full play of the enhancing effects of CNTs in nanotube-containing composites depends upon two preconditions, that is, the dispersibility of CNTs and their ability to tightly bind to each phase in the composite, which are determined by the chemical activity of CNTs.[33] It is well-known that the chemical reactivity of CNTs is mainly related to surface characteristics involving functional groups attached to CNT sidewalls, defects in tube-wall structure and surface crystallinity. Therefore, the theoretical and comparative analysis of the surface characteristics of the C-CNTs and F-CNTs could provide a better understanding of the above experimental results.

Generally, regular C-CNTs demonstrate such characteristics as an intact tubular structure with high crystallinity and few defects in the sidewalls.[34−36] In contrast, the present F-CNTs possess low crystallinity and a great number of defects, as shown in Figure 8. These unique microstructures are considered to be induced by special flaming conditions including: (1) synthesis in the atmosphere in which oxygen and nitrogen are abundant; (2) an unstable supply of carbon resources; and (3) thermal nonuniformity in the flame without protection from airflow.[20,21,23,37] Therefore, the inherent defects in the sidewalls of the F-CNTs are apt to be oxidized as two functional groups (−COOH and −CH_2OH).[20,38]

To comparatively evaluate the effect of surface activities of the F-CNTs and C-CNTs upon their bonding ability in composites, theoretical calculations based on molecular dynamics method were performed. In general, an MWCNT is considered to be composed of a number of SWCNTs in a coaxial geometry with weak intershell interaction and the outmost shell absorbing the functional groups. To simplify the CNT model, an armchair (8, 8) tube was chosen for calculating the structural energy of the C-CNTs and F-CNTs, where the former were assumed to be pristine armchair (8, 8) tubes without defects whereas the latter were assumed to be functionalized (8, 8) tubes with two atom vacancies and two chemical groups (−COOH and −CH_2OH) covalently attached at the sidewalls,[39] as shown in Figure 9.

The calculation results indicate that the bond energy distribution of the F-CNT are quite different from those of the C-CNT, as listed in Table 1. Due to its intact hexagonal carbon layer (graphite structure), the C-CNT is stable with a relatively low energy, which results in a chemical unreactiveness similar to that of graphite. Therefore, the C-CNT has limited ability regarding charge transfer and chemical interaction for the GFRP interface modification.

In contrast, the F-CNT is unstable and has higher total energy because of the atom vacancies and chemical groups. The high

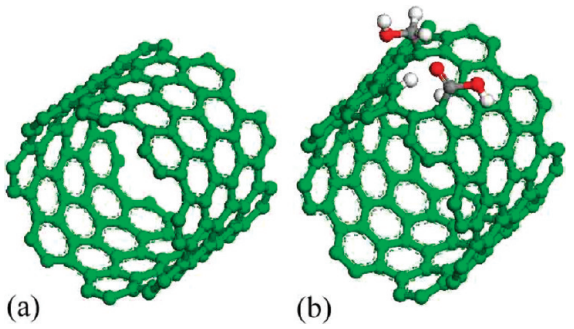

Figure 9. Schematic atomic structures of CNTs after geometry optimization: (a) (8, 8) CNT as the model of C-CNTs; (b) (8, 8) CNT with two defects and two functional groups as the model of F-CNTs.

Table 1. Energy Status of C-CNTs and F-CNTs

		valence energy (eV)				
CNTs	total energy (ev)	bond	angle	torsion	inversion	van der Waals (eV)
C-CNTs	34.48382	3.56293	0.16157	12.67084	0.50246	17.58609
F-CNTs	37.90511	3.95325	0.82500	15.26541	0.50259	17.35882

density of these groups combined with the great number of vacancies causes distortions of the hexagonal network and more carbon dangling bonds in a surface graphite layer, which results in localized disruption of conjugated π bonds and partial electron charge transfer from π bonds to carbon atoms in the sidewall and subsequently increases chemical reactivity.[18,40]

In brief, the F-CNT overcoating at the GFRP interface enables strong and direct interaction between the matrix and fibers, which greatly improves the fiber/matrix interphase cohesion and prevents initiation and propagation of microcracks. In addition, the alcohol (−CH_2OH) and carboxyl (−COOH) groups on their surface provide the F-CNTs with an intrinsic polarity, which contributes to their homogeneous dispersion at the fiber/matrix interface.

4. CONCLUSIONS

Fiber/matrix interface modification with CNTs is an effective approach to improve the shock resistance of GFRP composites. Compared with regular C-CNTs from a CVD process, the F-CNTs from ethanol flames have preferable chemical reactivity and good dispersibility due to a great number of defects and chemical groups in the sidewalls. Interface reinforcement with the F-CNTs effectively promotes the fiber/matrix interfacial cohesion strength and greatly increases the shock strength of GFRP. The unique surface characteristic of the F-CNTs is created during the flaming process, and no complicated post-treatment is required; hence, the structural and mechanical integrity of the CNTs are guaranteed. In addition, as the flaming synthesis is simpler, easier to control and less costly, the F-CNTs exhibit great potential for broader application in GFRP interface enhancement.

AUTHOR INFORMATION

Corresponding Author

*Tel.: +86-27-6875-2969 (C.P.). Fax: +86-27-6875-2003 (C.P.). E-mail: cxpan@whu.edu.cn (C.P.); kmliew@cityu.edu.hk (K.M.L.).

■ ACKNOWLEDGMENT

This work was supported by the Specialized Research Fund for the Doctoral Program of Higher Education (SRFDP 2007-0486016), Ministry of Education, China, and the National Basic Research Program of China (973 Program) (2009CB939705).

■ REFERENCES

(1) You, Y. J.; Park, Y. H.; Kim, H. Y.; Pak, J. S. *Compos. Struct.* **2007**, *80*, 117–122.
(2) Sela, N.; Ishai, O. *Composites* **1989**, *20*, 423–35.
(3) Compston, P.; Jar, P. Y. B.; Burchill, P. J.; Takahashi, K. *Appl. Compos. Mater.* **2002**, *9*, 291–314.
(4) Pham, S.; Burchill, P. J. *Polymer* **1995**, *36*, 3279–3285.
(5) Cheng, T. H.; Jones, F. R.; Wang, D. *Compos. Sci. Technol.* **1993**, *48*, 89–96.
(6) Zinck, P.; Maeder, E.; Gerard, J. F. *J. Mater. Sci.* **2001**, *36*, 5245–5252.
(7) Plueddemann, E. P. *Silane Coupling Agents*, 2nd ed.; Plenum Press: New York, 1999.
(8) Zhu, J.; Kim, J. D.; Peng, H. Q.; Margrave, J. L.; Khabashesku, V. N.; Barrera, E. V. *Nano Lett.* **2003**, *3*, 1107–1113.
(9) Bower, C.; Rosen, R.; Jin, L.; Han, J.; Zhou, O. *Appl. Phys. Lett.* **1999**, *74*, 3317–3319.
(10) Gong, X. Y.; Liu, J.; Baskaran, S.; Voise, R. D.; Young, J. S. *Chem. Mater.* **2000**, *12*, 1049–1052.
(11) Zhu, J.; Imam, A.; Crane, R.; Lozano, K.; Khabashesku, V. N.; Barrera, E. V. *Compos. Sci. Technol.* **2007**, *67*, 1509–1517.
(12) Bao, Q. L.; Zhang, H.; Yang, J. X.; Wang, S.; Tang, D. Y.; Jose, R.; Ramakrishna, S.; Lim, C. T.; Loh, K. P. *Adv. Funct. Mater.* **2010**, *20*, 782–791.
(13) Das, B.; Prasad, K. E.; Ramamurty, U.; Rao, C. N. R. *Nanotechnology* **2009**, *20*, 125705.
(14) Stevens, J. L.; Huang, A. Y.; Peng, H. Q.; Chiang, I. W.; Khabashesku, V. N.; Margrave, J. L. *Nano lett.* **2003**, *3*, 331–336.
(15) Riggs, J. E.; Guo, Z.; Carroll, D. L.; Sun, Y. P. *J. Am. Chem. Soc.* **2000**, *122*, 5879–5880.
(16) Sun, Y. P.; Huang, W.; Lin, Y.; Fu, K.; Kitaigorodsky, A.; Riddle, L. A.; Yu, Y. J.; Carroll, D. L. *Chem. Mater.* **2001**, *13*, 2864–2869.
(17) Georgakilas, V.; Tagmatarchis, N.; Pantarotto, D.; Bianco, A.; Briand, J. P.; Prato, M. *Chem. Commun.* **2002**, 3050–3051.
(18) Niyogi, S.; Hamon, M. A.; Hu, H.; Zhao, B.; Bhowmik, P.; Sen, R.; Itkis, M. E.; Haddon, R. C. *Acc. Chem. Res.* **2002**, *35*, 1105–1113.
(19) Chen, J.; Hamon, M. A.; Hu, H.; Chen, Y. S.; Rao, A. M.; Eklund, P. C.; Haddon, R. C. *Science* **1998**, *282*, 95–98.
(20) Bao, Q. L.; Zhang, J.; Pan, C. X.; Li, J.; Li, C. M.; Zang, J. F.; Tang, D. Y. *J. Phys. Chem. C* **2007**, *111*, 10347–10352.
(21) Pan, C. X.; Liu, Y. L.; Cao, F.; Wang, J. B.; Ren, Y. Y. *Micron* **2004**, *35*, 461–468.
(22) Bao, Q. L.; Bao, S. J.; Li, C. M.; Qi, X.; Pan, C. X.; Zang, J. F.; Lu, Z. S.; Li, Y. B.; Tang, D. Y.; Zhang, S.; Lian, K. *J. Phys. Chem. C* **2008**, *112*, 3612–3618.
(23) Bao, Q. L.; Pan, C. X. *Nanotechnology* **2006**, *17*, 1016.
(24) Qi, X.; Bao, Q. L.; Li, C. M.; Gan, Y.; Song, Q.; Pan, C. X.; Tang, D. Y. *Appl. Phys. Lett.* **2008**, *92*, 113113.
(25) Bao, Q.; Zhang, H.; Pan, C. *Appl. Phys. Lett.* **2006**, *89*, 063124.
(26) Bao, Q.; Ran, X.; Zhang, H.; Qi, X.; Fu, Q.; Pan, C. X. *New Carbon Mater.* **2008**, *23*, 44–50.
(27) Wang, X.; Liu, H. M.; Fang, P. F.; Liao, L. M.; Pan, C. X.; Liew, K. M. *J. Nanosci. Nanotechnol.* **2010**, *10*, 948–955.
(28) Liu, Y. L.; Fu, Q.; Pan, C. X. *Carbon* **2005**, *43*, 2264–2271.
(29) Cicala, G.; Cristaldi, G.; Recca, G.; Ziegmann, G.; ElSabbagh, A.; Dickert, M. *AIP Conf. Proc.* **2008**, *1042*, 263–265.
(30) Omata, Y.; Yamagami, Y.; Tadano, K.; Miyake, T.; Saito, S. *Phys. E* **2005**, *29*, 454–468.
(31) Schwartz, H. S.; Hartness, J. T. In *Toughened Composites*; ASTM STP; Johnston, N. J., Ed.; American Society for Testing and Materials: Philadelphia, PA, 1987; Vol. 937.
(32) Dzenis, Y. A.; Reneker, D. U.S. Patent 6 265 333, 2001.
(33) Chen, Y.; Haddon, R. C.; Fang, S.; Rao, A. M.; Eklund, P. C.; Lee, W. H.; Dickey, E. C.; Grulke, E. A.; Pengdergrass, J. C.; Chavan, A.; Haley, B. E.; Smalley, R. E. *J. Mater. Res.* **1998**, *13*, 2423–2431.
(34) Bonnota, A. M.; Deldema, M.; Beaugnonb, E.; Fournier, T.; Schouler, M. C.; Mermoux, M. *Diamond Relat. Mater.* **1999**, *8*, 631–635.
(35) Lee, C. J.; Park, J.; Huh, Y.; Lee, J. Y. *Chem. Phys. Lett.* **2001**, *343*, 33–38.
(36) Zou, X. P.; Abe, H.; Shimizu, T.; Ando, A.; Nakayama, Y.; Tokumoto, H.; Zhu, S. M.; Zhou, H. S. *Phys. E* **2004**, *24*, 14–18.
(37) Pan, C. X.; Xu, X. R. *J. Mater. Sci. Lett.* **2002**, *21*, 1207–1209.
(38) Lee, S. M.; Lee, Y. H.; Hwang, Y. G.; Hahn, J. R.; Kang, H. *Phys. Rev. Lett.* **1999**, *82*, 217–220.
(39) Wang, C. C.; Zhou, G.; Liu, H. T.; Wu, J.; Qiu, Y.; Gu, B. L.; Duan, W. H. *J. Phys. Chem. B* **2006**, *110*, 10266–10271.
(40) Cheng, H. M. *Carbon Nanotubes Synthesis, Microstructure, Properties and Applications*; Chemical Industry Press: Beijing, 2002 (in Chinese).